



# Direct measurement of electron drift parameters of wide band gap semiconductors

Z. He\*, G.F. Knoll, D.K. Wehe

*Department of Nuclear Engineering and Radiological Sciences, University of Michigan, Ann Arbor, MI 48109-2104, USA*

Received 16 January 1998

## Abstract

This paper describes a novel technique developed for directly measuring the electron mean free drift time  $\tau_e$  in wide band gap semiconductors. This method is based on a newly developed digital data analysis system, in conjunction with single polarity charge sensing, depth sensing and radial sensing techniques. Compared with conventional methods, the new technique does not involve curve fitting, allows the use of high-energy  $\gamma$ -rays, and is not sensitive to ballistic deficit nor the non-uniform electric field within semiconductors. © 1998 Elsevier Science B.V. All rights reserved.

## 1. Introduction

Charge transport properties are important characteristics of semiconductors. In particular, they are among the most important parameters which determine detector performance when semiconductors are used as  $\gamma$ -ray detectors. This is because large detector volume is required for efficient  $\gamma$ -ray detection and good charge transport properties are essential for  $\gamma$ -ray spectroscopy. Wide band gap semiconductors, such as CdZnTe, CdTe and HgI<sub>2</sub>, are attractive materials for room-temperature  $\gamma$ -ray detectors. But the poor hole trapping properties are the major problem which has hindered the application of these materials for more than two decades. Single polarity charge sensing [1] has shown the potential for avoiding this problem since the signal

induced by holes can be eliminated. However, since electrons are also trapped in these wide band gap semiconductors, the detector performance that can be achieved in single polarity charge sensing devices is determined mainly by electron transport properties.

Conventional methods [2] of measuring electron mobility  $\mu_e$  and mean free drift time  $\tau_e$  product  $\mu_e\tau_e$  are based on the Hecht relation [3]:

$$Q = N_0 e_0 \frac{\lambda_e}{D} \left( 1 - \exp\left(-\frac{D}{\lambda_e}\right) \right), \quad (1)$$

where  $Q$  is the induced charge on one of the planar electrodes (cathode or anode),  $N_0$  is the number of electron-hole pairs generated by the  $\gamma$ -ray,  $e_0$  is the charge of an electron,  $\lambda_e$  is the mean free drift length of the electron and  $D$  is the thickness of the semiconductor.  $\lambda_e$  is defined as

$$\lambda_e = \mu_e \tau_e E, \quad (2)$$

\* Corresponding author. Tel.: +1 313 764 5285; fax: +1 313 763 4540; e-mail: hezhong@engin.umich.edu.

where  $E$  is the electric field intensity and is assumed to be constant within the bulk of the material,  $E = V/D$  for a device using planar electrodes, where  $V$  is the bias voltage between the cathode and the anode.

In conventional measurements of electron transport properties, electron–hole pairs are generated very close to the cathode surface so that the induced signal is from the drift of electrons only. This can be implemented by using a pulsed laser,  $\alpha$  particles, or a low-energy hard X-ray source incident from the cathode surface. By measuring the variation of photopeak amplitude (which are assumed to be proportional to the total induced charge  $Q$  of Eq. (1)) as a function of  $V$ , the  $\mu_e\tau_e$  product can be obtained from a curve-fitting procedure using Eqs. (1) and (2). The electron mobility can be independently determined from a measurement of electron drift velocity, and  $\tau_e$  deduced.

Several factors may distort such measurement results. For example, one of the assumptions is that the measured pulse amplitudes are proportional to the total-induced charge  $Q$  at different bias voltages. This is only true when the shaping time constant is much longer than the pulse rise time determined by the electron drift time across the detector thickness. In practice, this condition cannot be met in many cases and a correction for ballistic deficit has to be performed. Another assumption is that the electric field is constant and charge trapping is uniform within the bulk. In practice, the electric field may not be constant due to the presence of space charge. Furthermore, the charge trapping conditions at surfaces may be significantly different from those within the bulk. If electron–hole pairs are only generated very near the cathode surface, the measurement results may be affected by surface trapping conditions. Finally, the value of  $\mu_e\tau_e$  cannot be obtained directly from the measurement data, but rather a curve-fitting procedure must be employed to give an estimate of  $\mu_e\tau_e$ . Among the systematic errors mentioned above, ballistic deficit and surface trapping tend to produce a bias toward lower observed values of  $\mu_e\tau_e$ .

This paper describes an alternative approach in which  $\tau_e$  can be directly measured. This method performs digital data analysis of pulse waveforms captured at the outputs of preamplifiers, uses single

polarity charge sensing [1] to measure the number of electrons arriving at the anode surface, employs depth sensing [4,5] to provide the electron drift distance and radial sensing [6] to reduce measurement error from edge effects. This method allows the use of high-energy  $\gamma$ -ray sources so that the electron–hole pairs can be generated throughout the bulk of the detector rather than concentrated near the cathode surface. Possible systematic errors from ballistic deficit can be eliminated using this approach.

## 2. Digital data analysis system

The measurement system is schematically shown in Fig. 1. The semiconductor crystal is fabricated with a coplanar grid structure on the anode. A Tektronix TDS 744A digital oscilloscope is used to digitize pulse waveforms at the outputs of preamplifiers connected to the collecting anode, non-collecting anode and the cathode. During each cycle, pulse waveforms of 50 events are captured continuously and stored in the memory of the oscilloscope, and then transferred together to a PC through a GPIB interface. A Labview program performs digital data analysis, such as digital pulse shaping for  $\gamma$ -ray spectroscopy, electron drift time measurement, depth sensing and radial sensing. The system is a quasi-real-time system since it only misses events during its data transfer and processing period. With this system, waveforms of  $\gamma$ -ray events having particular characteristics, such as

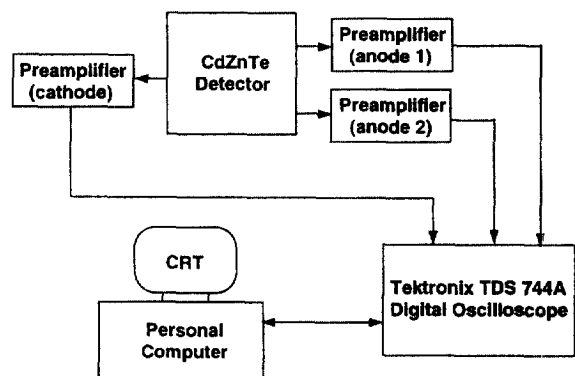


Fig. 1. The digital data analysis system based on the use of a Tektronix TDS 744A digital oscilloscope.

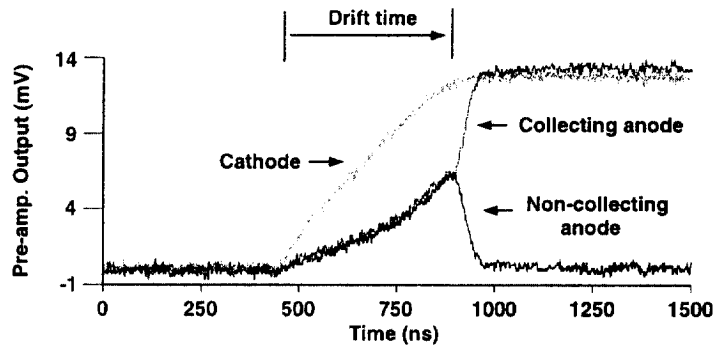


Fig. 2. Pulse waveforms obtained from the outputs of preamplifiers by the digital oscilloscope. The  $\gamma$ -ray interaction location was near the cathode surface.

a specified  $\gamma$ -ray energy deposition at a given interaction depth, can be analyzed.

The waveforms of a typical  $\gamma$ -ray event whose interaction location is near the cathode surface are shown in Fig. 2. The time interval between the beginning of the pulse and the turning point from positive increase to negative drop of the signal of the non-collecting anode is defined as electron drift time  $t_{\text{drift}}$ . During this time, electrons have drifted from near the surface of the cathode to a distance  $P$  from the anode surface, where  $P$  is the pitch of the coplanar anodes and is typically much smaller than the detector thickness  $D$ .

### 3. Depth sensing

Pulse amplitudes from the coplanar anodes and the cathode are obtained using digital pulse shaping. Currently, pulse amplitudes are determined simply by the difference of the average pulse waveform amplitudes before the beginning of the signals and after the electrons are collected. The  $\gamma$ -ray interaction depth  $z$  is obtained using the method reported in our earlier papers [4,5]:

$$z = C/(A1 - A2),$$

where  $C$  is the cathode pulse amplitude and  $(A1 - A2)$  is the difference signal from the coplanar anodes when their relative gain is 1.0.

Although some non-linear effects could exist, the measured depth parameter  $C$  is a monotonic function of the true depth [5]. Therefore, when we

obtain the distribution of the depth parameter using  $\gamma$ -rays which deposited all their energy within the detector, events having the maximum value of  $C$  must originate from near the cathode surface and those having small values of  $C$  are from near the anode surface. Using this technique,  $\gamma$ -ray events originating from a specific depth can be selected for measurements.

### 4. Radial sensing

In addition to the depth sensing, a radial sensing technique is also implemented on our system. The employment of a third boundary electrode, which surrounds the central coplanar anodes and is biased at a potential up to the potential of the non-collecting anode, makes the radial sensing possible. The detailed introduction of the boundary electrode is described elsewhere [6]. Since the boundary electrode is located near the periphery of the anode surface, it shares more induced charge when electrons are drifting toward anodes near the sides of the detector, and less when electrons are moving in the central region of the crystal. Therefore, the signal difference between the total induced charge of central anodes ( $A1 + A2$ ) and that of the cathode (which equals the sum of the induced charges of boundary electrode and central anodes) can indicate the relative radial location of  $\gamma$ -ray interactions. The radial parameter  $R$  is calculated as

$$R = \frac{1}{n} \sum_{t=0}^{t_{\text{anis}}} (C - (A1 + A2))^2,$$

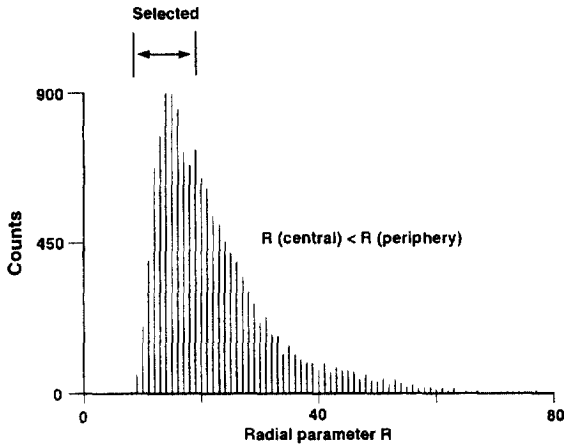


Fig. 3. The measured distribution of the radial parameter  $R$  of 662 keV  $\gamma$ -rays originating from near the cathode surface. Events with  $R \leq 20$  were selected for the mobility and mean free drift time measurements.

$n$  is the number of digitized samples during electron drift time. Although the calibration of the radial parameter  $R$  in terms of the actual radial position has not been performed, the relative location  $R(\text{central}) < R(\text{periphery})$  was verified from experiments [6]. As an example, Fig. 3 shows the distribution of radial parameter  $R$  from  $\gamma$ -ray events originating near the cathode surface obtained from a 1 cm cube CdZnTe detector.

Since electrons must reach the collecting anode inside the boundary electrode, events from the periphery have a longer electron trajectory than those from the central region if they started from the same depth. In order to reduce systematic error due to different electron drift lengths, events originating from the central region were selected for our measurements of drift properties. The selected events typically account for about half of the total events originating from the same depth.

## 5. Measurement of electron mobility $\mu_e$

The measured distributions of electron drift time from a 1 cm cube CdZnTe detector at three bias voltages are shown in Fig. 4. The cathode voltages relative to that of the non-collecting anode were 1, 2 and 2.6 kV, respectively. Since the voltage be-

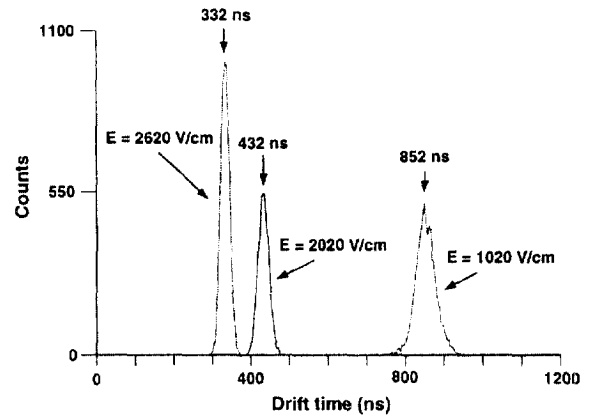


Fig. 4. Drift time distributions of electrons across a thickness of 0.95 cm CdZnTe at three average electric field intensities  $E$ . Centroid drift times are shown with arrows.

tween the collecting and non-collecting anodes was 40 V, the average electric field intensity within the bulk can be approximated as 1020, 2020 and 2620 V/cm, respectively [7]. From the distributions of drift time shown in Fig. 4, one can see that the electron drift is quite uniform within the bulk of CdZnTe.

The electron mobility  $\mu_e$  can be obtained from the measurement of electron drift time  $t_{\text{drift}}$  as

$$\mu_e = \frac{z_{\text{drift}}}{E \cdot t_{\text{drift}}}.$$

It should be noted that the drift length  $z_{\text{drift}}$  on this 1 cm thick CdZnTe detector is 0.95 cm, since the pitch of the coplanar anodes on this device is  $\sim 500 \mu\text{m}$  [7]. From the detector used in this example, the centroid drift times measured at the three bias voltages shown in Fig. 4 all give electron mobilities  $\sim 1.1 \times 10^3 \text{ (cm}^2/\text{V s)}$ . This result means that the electron mobility  $\mu_e$  is observed to be constant over a range of electric field magnitude from 1 to  $\sim 3 \text{ kV/cm}$ .

## 6. Direct measurement of $\tau_c$ by relative measurements

In the presence of uniform trapping, the number of electrons  $N(t)$  surviving after a drift time  $t$  can be

expressed as

$$N(t) = N_0 \exp\left(-\frac{t}{\tau_e}\right). \quad (3)$$

Our measurement procedure for measuring  $\tau_e$  is based on the unique property that, when the relative gain between the coplanar anodes is set to be 1.0, the coplanar difference signal depends only on the number of collected electrons, and not on their drifting distance. The peak amplitudes  $N_1$  and  $N_2$  obtained from the coplanar signal for two different bias voltages  $V_1$  and  $V_2$  are recorded only for interactions that occur near the cathode surface. Since the electron drift times  $t_1$  and  $t_2$  are different in the two cases, from Eq. (3):

$$N_1 = N_0 \exp(-t_1/\tau_e), \quad (4)$$

$$N_2 = N_0 \exp(-t_2/\tau_e). \quad (5)$$

$$\frac{\sigma(\tau_e)}{\tau_e} = \sqrt{\frac{\sigma^2(t_1) + \sigma^2(t_2)}{(t_1 - t_2)^2} + \frac{1}{\ln^2(N_1/N_2)} \cdot \left[ \left(\frac{\sigma(N_1)}{N_1}\right)^2 + \left(\frac{\sigma(N_2)}{N_2}\right)^2 \right]}. \quad (8)$$

We have

$$N_2 = N_1 \exp\left(-\frac{t_2 - t_1}{\tau_e}\right), \quad (6)$$

$$\tau_e = \frac{t_2 - t_1}{\ln(N_1/N_2)}. \quad (7)$$

Since the electron drift time and the photopeak amplitude are measured simultaneously, the electron mean free drift time  $\tau_e$  can be obtained directly from our measurement data.

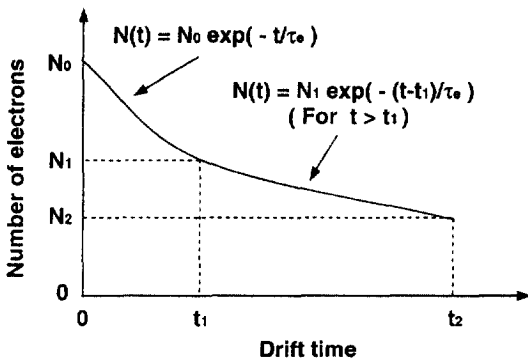


Fig. 5. Illustration of the principle for measuring  $\tau_e$ .

Eq. (6) shows that we do not have to measure the original electron-hole pairs  $N_0$  generated by the  $\gamma$ -ray interaction. The electron mean free drift time  $\tau_e$  can be obtained by measuring the relative electron transmission  $N_2/N_1$  during electron drift time ( $t_2 - t_1$ ). This principle is illustrated in Fig. 5.

As an example, Fig. 6 shows the energy spectra of 662 keV  $\gamma$ -rays obtained at bias voltages of 1 and 2 kV from a 1 cm cube CdZnTe detector. In both cases, the  $\gamma$ -ray interactions were restricted to be near the cathode surface using the depth sensing technique. The centroids of the two photopeak amplitudes were used as  $N_1$  and  $N_2$  in Eq. (7).

## 7. Error estimation

From Eq. (7), the measurement error of  $\tau_e$  can be estimated using the error propagation:

To a good approximation, we can assume that both the electron drift time and  $\gamma$ -ray photopeak amplitudes at a fixed bias voltage follow Gaussian distributions. Therefore, the standard deviation of the centroid  $\sigma(\text{centroid})$  of a Gaussian distribution can

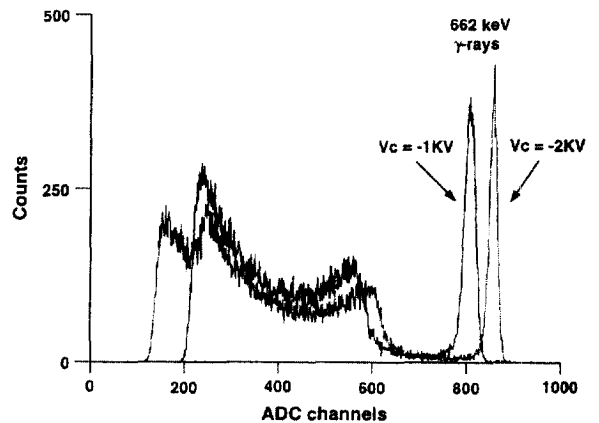


Fig. 6. Energy spectra of 662 keV  $\gamma$ -rays at 1 and 2 kV bias voltages between the cathode and the anode. Both spectra were obtained from events with interaction locations near the cathode surface. The detector is a 1 cm cube of CdZnTe and  $V_{a1-a2} = +40$  V.

be obtained from the standard deviation  $\sigma$  (Gaussian) of the Gaussian distribution and the total event number  $M$ :

$$\sigma(\text{centroid}) = \frac{\sigma(\text{Gaussian})}{\sqrt{M}} \quad (9)$$

In practice,  $\sigma(t_1), \sigma(t_2), \sigma(N_1)$  and  $\sigma(N_2)$  can be obtained from the FWHMs and the total event numbers of the measured distributions of electron drift time and photopeak amplitude.

For example, the electron drift time distribution and energy spectra of events originated near the cathode surface of a 1 cm cube CdZnTe detector are shown in Fig. 4 and Fig. 6. The FWHMs are 52 and 36 ns for measured electron drift time distributions at 1 and 2 kV bias voltages, respectively. With  $\sim 10000$  event number, the  $\sigma(t_1)$  and  $\sigma(t_2)$  are estimated to be 0.22 and 0.15 ns (Note:  $\sigma \approx \text{FWHM}/2.35$ ). The centroids of photopeak amplitudes are 808 and 858 ADC channels, and the FWHMs are 26 and 18 ADC channels, respectively. We get:

$$\frac{\sigma(N_1)}{N_1} = \frac{26}{2.35 \times 808 \times \sqrt{10000}} \approx 1.37 \times 10^{-4}$$

similarly,

$$\frac{\sigma(N_2)}{N_2} = 0.89 \times 10^{-4}$$

and  $\ln(N_1/N_2) \approx 0.06$ . These results yield:

$$\frac{\sigma^2(t_1) + \sigma^2(t_2)}{(t_1 - t_2)^2} \approx 0.4 \times 10^{-6},$$

$$\left( \frac{1}{\ln(N_1/N_2)} \right)^2 \cdot \left[ \left( \frac{\sigma(N_1)}{N_1} \right)^2 + \left( \frac{\sigma(N_2)}{N_2} \right)^2 \right]$$

$$\approx 7.41 \times 10^{-6}.$$

Substitute these values into Eq. (8), we have

$$\frac{\sigma(\tau_e)}{\tau_e} \approx 0.27\%.$$

This estimate shows that the new method could provide very good precision in electron mean free drift time measurements. In practice, systematic errors may dominate the measurement precision, such as the error in electron drift time measurement due to the limited depth resolution of the technique. At a  $\gamma$ -ray energy of 662 keV, typical depth resolution is a few percent of the detector thickness [5]. This could limit the measurement precision on  $\tau_e$  to a few percent.

## 8. Measurement results

Four CdZnTe detectors have been fabricated into coplanar grid single polarity charge sensing devices. The crystals were from eV Products [8]. The electron mobility  $\mu_e$  and mean free drift time  $\tau_e$  were measured using the technique described above, and the results are summarized in Table 1.

## 9. Discussion

Since the only parameter changed between two measurements is the bias voltage, which changes the electron drift time, many possible systematic errors are eliminated. These include the change in detector performance versus  $\gamma$ -ray interaction depth, non-uniformity of charge collection, variation of electron trajectories, etc. For example, there may be some deviation from unity of the relative gain between the coplanar anodes. This

Table 1  
Measurement results for  $\mu_e$  and  $\tau_e$

Detector (ID)	$\mu_e$ ( $10^3 \text{ cm}^2/\text{V s}$ )	$\tau_e$ ( $\mu\text{s}$ )	Bias (cathode–anode)
1 × 1 × 1 cm (704474Co)	1.1	7.00	1–2 kV
1.5 × 1.5 × 0.5 cm (L1643 #1)	1.3	5.51	200–400 V
1.5 × 1.5 × 1 cm (700033)	1.0	4.02	800–1 kV
1 × 1 × 1 cm (1315-04)	1.0	6.93	1–2 kV

relative gain would produce a depth-dependent gain for the pulse amplitudes. Since we collect  $\gamma$ -ray events only from near the cathode surface, this effect can be cancelled by this relative measurement.

The new technique, which directly measure electron  $\mu_e$  and  $\tau_e$ , are based on the combination of single polarity charge sensing and depth sensing methods. They allow the use of high-energy  $\gamma$ -rays to avoid possible errors caused by different trapping properties on the surface and within the bulk. They take advantage of the good signal-to-noise ratio of measurements using  $\gamma$ -rays at high energies, and do not require the use of a vacuum system as when  $\alpha$  irradiation is used. However, the new techniques could be used in conjunction with  $\alpha$  sources, in which case no depth sensing would be necessary if the  $\alpha$ -particles are incident from the cathode surface. These techniques could also be used on other types of wide band-gap semiconductors, such as  $\text{HgI}_2$  and  $\text{CdTe}$ . Furthermore, if a significant number of holes can travel across the semiconductor thickness with sufficient mobility, the new technique could be used to measure  $\mu_h$  and  $\tau_h$ . The major restriction is that single polarity charge sensing must be employed.

## Acknowledgements

We would like to thank Dr. D.S. McGregor for useful discussions. This work was supported under the US Department of Energy, Grant No. DOE-FG08-94NV11630.

## References

- [1] P.N. Luke, *Appl. Phys. Lett.* 65 (22) (1994) 2884.
- [2] T.E. Schlesinger, R.B. James (Eds.), *Semiconductors for Room Temperature Nuclear Detector Applications*, *Semiconductors and Semimetals*, vol. 43, Academic Press, New York, 1995, pp. 493–530.
- [3] K. Hecht, *Z. Phys. (Germany)* 77 (1932) 235.
- [4] Z. He, G.F. Knoll, D.K. Wehe, R. Rojeski, C.H. Mastrangelo, M. Hammig, C. Barrett, A. Uritani, *Nucl. Instr. and Meth. A* 380 (1996) 228–231.
- [5] Z. He, G.F. Knoll, D.K. Wehe, J. Miyamoto, *Nucl. Instr. and Meth. A* 388 (1997) 180–185.
- [6] Z. He, G.F. Knoll, D.K. Wehe, Y.F. Du, *Nucl. Instr. and Meth. A* 411 (1998) 107.
- [7] Z. He, *Nucl. Instr. and Meth. A* 365 (1995) 572–575.
- [8] eV Products, 375 Saxonburg Boulevard, Saxonburg, PA 16056, USA.